Astron. Astrophys. 347, 919–926 (1999)

ASTRONOMY AND ASTROPHYSICS

Scattering polarization due to light source anisotropy

I. Large spherical envelope

M.B. Al-Malki[*]**, J.F.L. Simmons, R. Ignace, J.C. Brown, and D. Clarke**

Kelvin Bldg, Department of Physics and Astronomy, University of Glasgow, Glasgow, G12 8QQ, Scotland, UK

Received 21 January 1999 / Accepted 20 April 1999

Abstract. Expressions are developed for the flux and polarization of radiation scattered by a spherically symmetric envelope for a central point stellar light source that radiates anisotropically. These are obtained in terms of the components of the spherical harmonics of the flux anisotropy from the source. Such anisotropy can arise from stellar spots, or from distortion of the star through rotation, pulsation, or magnetic effects. Explicit expressions for the Stokes parameters are obtained in the case of an ellipsoidal star of uniform surface brightness. It is thus shown that even when the scattering envelope is spherical, observationally significant polarization can arise from stars with physically realistic degrees of distortion. The time dependence of the polarization is computed for models of ellipsoidal stars in the cases of pure rotation, pure pulsation, and both rotation and pulsation.

Key words: polarization – stars: binaries: general – stars: circumstellar matter – stars: oscillations – stars: rotation

1. Introduction

Following the first general analytic treatment by Brown & McLean (1977) of polarization of starlight from an unpolarized isotropic point light source produced by single scattering of electrons in an axisymmetric circumstellar envelope, of otherwise arbitrary shape, Brown et al. (1978) treated the case of multiple light sources in optically thin envelopes of arbitrary shape and applied the theory to rotating binary systems (c.f., also Rudy & Kemp 1978). Cassinelli et al. (1987) and Brown et al. (1989) incorporated the effects of the finite size of the star as a light source. Milgrom (1978), Brown & Fox (1989), Fox & Brown (1991), and Fox (1991) considered the consequences of occultation effects by the star for the observed polarization of circumstellar envelopes. Simmons (1982, 1983) generalized the work of Brown & McLean (1977) and of Brown et al. (1978) to Mie scattering in anisotropic envelopes. However, in all of these preceding works, the light source has been treated as an isotropic unpolarized emitter.

Some special cases of anisotropic light source have been considered. For example, Gnedin et al. (1976) calculated the polarization for close X-ray binaries using a two dimensional model of an ellipsoidal Roche lobe. Stamford & Watson (1980) calculated the polarization produced by nonradially pulsating stars. Fox (1993) showed how to compute the envelope polarization when the stellar source is itself intrinsically polarized. He even considered the scattering of polarized light from a stellar source of arbitrary shape using an approach based on intensity moments. His applications, however, were restricted to a spherical star with limb polarization. Bjorkman & Bjorkman (1994) have considered the effects of gravity darkening in a rapidly rotating star for the UV continuum polarization of an axisymmetric disk. In this first paper, we derive the effects of anisotropy of the stellar light source using the formalism of Simmons (1982, 1983). Here we consider the case of a spherical envelope to isolate the basic effects arising from stellar anisotropy, leaving more general cases to later papers in the series.

Stars are in general anisotropic light sources. This anisotropy arises mainly through two effects. First, the surface brightness may be non-uniform owing to blemishes, for example from magnetic fields, spots, or convection cells. Second, the star may be non-spherical, the distortion arising from rotation, pulsation, magnetic fields, or tidal effects of a companion star. In such cases the polarization that is produced in the optically thick stellar atmosphere is small unless the distortion is quite significant (Haisch & Cassinelli 1976; Collins & Buerger 1974). The small level of polarization from such atmospheres is largely due to multiple scattering, which tends to destroy polarization. Furthermore, the symmetry of the stellar surface produces cancellation and a low integrated polarization. On the other hand, single scattering from an optically thin envelope may produce significant polarization.

In the following section, we derive exact expressions for the Stokes parameters for anisotropic light sources with spherical envelopes and Thomson or Rayleigh scattering. In Sect. 3, the general expressions are applied to the specific case of an ellipsoidal star of uniform brightness, and in Sect. 4, these results are used to compute the polarization expected from rotating stars, X-ray binaries, and non-radially pulsating stars.

Send offprint requests to: rico@astro.gla.ac.uk

[*] Now at P.O. Box 87946, Riyadh 11652, Saudi Arabia

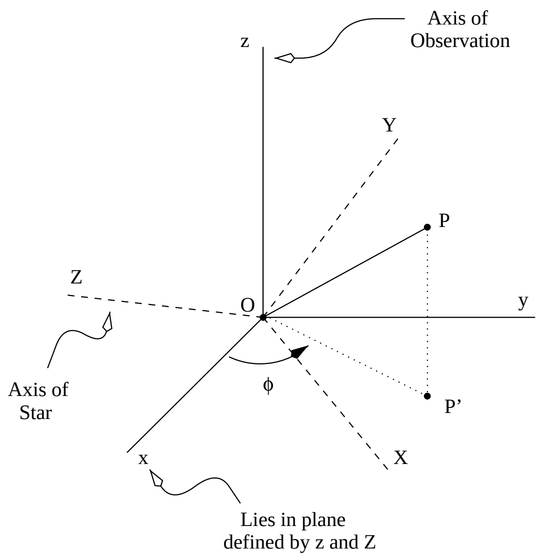

Fig. 1. Definitions of the star and the observer coordinates. The point O marks the emitting anisotropic star (point source), and P a general scattering point in the envelope. OZ is the rotation axis, where θ is the scattering angle, and ϕ is the polarization direction. The Euler angles are $\alpha = 0$, $\beta = i$ the inclination angle between Oz and OZ, and $\gamma = \phi_{\rm s}$ the angle to the X-axis in the xy-plane. The scattering plane is $P'OP$.

2. The polarization arising from source anisotropy

We derive the general case of Rayleigh or Thomson scattering in a circumstellar envelope, with the star located at its center. Following, we restrict ourselves to a spherical envelope to illustrate the basic effects of source anisotropy. For simplicity it is assumed that the star is small compared to the size of the envelope, thus allowing each scattering particle to be treated as being illuminated by radiation from a unique direction. Hence, the effects of occultation (e.g., Fox & Brown 1991) and finite star depolarization (Cassinelli et al. 1987) are neglected. Even for a spherical envelope, the occurrence of non-isotropic illumination will lead to a net observed polarization, which will depend on the angle between the direction of maximum flux from the source and the line of sight.

We follow Simmons (1982, 1983) in using two coordinate frames centered on the star. Referring to Fig. 1, the star's frame (X, Y, Z) has spherical coordinates (r, ϑ, φ). The observer's frame is described by (x, y, z) with spherical coordinates (r, θ, ϕ). The axis Oz is directed toward the observer, and Ox is chosen so that OZ lies in the $x-z$ plane (see Fig. 1). The orientation of frame (X, Y, Z) to that of (x, y, z) is given by the Euler angles (α, β, γ) (c.f., Messiah 1962). With the adopted orientation of axes, the Euler angles are $\alpha = 0$, $\beta = i$ the viewing inclination angle between OZ and Oz, and $\gamma = \phi_{\rm s}$ is the angle between OX and the $x-z$ plane (or the longitude of the star). The angle $\phi_{\rm s}$ thus measures the rotational position of the star relative to the observer (see Fig. 2). Light scattered by an electron at position (r, ϑ, φ) in the star frame will be scattered through an angle θ in the observer's system, and the orientation of the scattering plane about z will be given by ϕ.

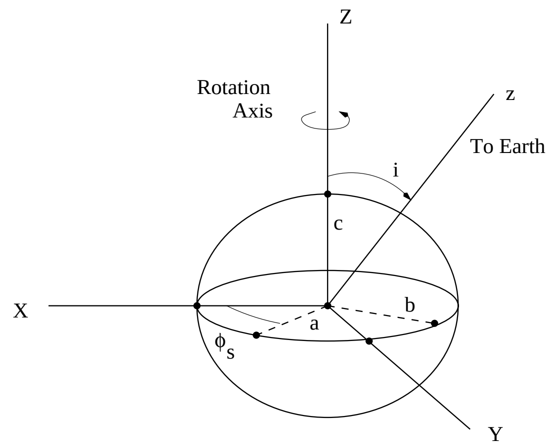

Fig. 2. The ellipsoidal star coordinate system, where the c-axis is along the Z-axis (i.e., the rotation axis).

In general the number density of scatterers may be written as $n(r, \theta, \phi)$ and the flux of unpolarized stellar radiation as $\mathcal{F}(r, \theta, \phi)$. Then following Simmons (1982), the scattered flux and Stokes parameters $(\mathcal{F}_{\rm sc}, Q, U)$ of the scattered radiation at the Earth a distance D away are given by

$$\left.\begin{array}{l}\mathcal{F}_{\rm sc}\\ Z^*\end{array}\right\} = \frac{1}{2k^2 D^2} \int\int\int n(r,\theta,\phi)\, \mathcal{F}(r,\theta,\phi)\, r^2 \times \left\{\begin{array}{l}(i_1+i_2)\\ (i_1-i_2)\exp(-2{\rm i}\phi)\end{array}\right. dr\, \sin\theta\, d\theta\, d\phi, \quad (1)$$

where $Z^* = Q - {\rm i}U$ with ${\rm i} = \sqrt{-1}$, $k = 2\pi/\lambda$ is the wave number, and i_1 and i_2 are the scattering functions as defined by van de Hulst (1957). The circular polarization will be taken as zero.

For Thomson scattering by free electrons or Rayleigh scattering, we have

$$i_1 \pm i_2 = \frac{3k^2}{8\pi}\, \sigma\, (1 \pm \cos^2\theta) \quad (2)$$

where σ is the total scattering cross section (e.g., see Brown & McLean 1977). For Thomson scattering σ is independent of the wave number k whereas for Rayleigh scattering $\sigma \propto k^4 \propto \lambda^{-4}$.

In relation to previous models, the basic result of source anisotropy is to introduce the factor $\mathcal{F}(r, \theta, \phi)$ inside the integral over the scattering volume. This complication of allowing both $\mathcal{F}$ and n to be anisotropic immediately suggests that the effects on Q and U will depend on whether the two functions enhance or offset one another. In the case of a spherical envelope, the problem simplifies owing to the number density being a function of radius only, with $n = n(r)$.

The illumination $\mathcal{F}(r, \theta, \phi)$ in Eq. (1) describes the stellar radiative properties in the observer's system of coordinates, but it is more natural to describe the behavior in terms of the stellar system. Providing that $\mathcal{F}$ varies smoothly, we may express it in terms of spherical harmonics, viz

$$\mathcal{F}(r, \vartheta, \varphi) = \sum_{l=0}^{\infty} \sum_{\rm m=-l}^{\rm m=l} F_{l\rm m}(r)\, Y_{l\rm m}(\vartheta, \varphi). \quad (3)$$

Using the rotation matrices described by Messiah (1962; c.f., Simmons 1983) to convert from the star's frame to the observer's, we have

$$Y_{l\mathrm{m}}(\vartheta,\varphi) = \sum_{\mathrm{n}=-l}^{\mathrm{n}=l} R^{(l)}_{\mathrm{nm}}(\alpha,\beta,\gamma)\, Y_{l\mathrm{n}}(\theta,\phi). \tag{4}$$

Substituting this into Eq. (3) yields the transformation of $\mathcal{F}$. Here, the required transformation is the one relating $\mathcal{F}$ in the star system to that for the observer's system:

$$\begin{aligned}\mathcal{F}(r,\theta,\phi) \;=\; & \sum_{l=0}^{\infty}\sum_{\mathrm{m}=-l}^{\mathrm{m}=l} F_{l\mathrm{m}}(r) \\ & \times \sum_{\mathrm{n}=-l}^{\mathrm{n}=l} R^{(l)}_{\mathrm{nm}}(\alpha,\beta,\gamma)\, Y_{l\mathrm{n}}(\theta,\phi).\end{aligned} \tag{5}$$

Note that $Y_{l\mathrm{n}}$ is defined as in Jackson (1975), viz

$$Y_{l\mathrm{n}}(\theta,\phi) = \kappa_{l\mathrm{n}}\, P^{\mathrm{n}}_l(\cos\theta) e^{\mathrm{i}\, n\phi} \tag{6}$$

with

$$\kappa_{l\mathrm{n}} = \sqrt{\frac{(2l+1)\,(l-n)!}{4\pi\,(l+n)!}} \tag{7}$$

and

$$P^{\mathrm{n}}_l(x) = (-1)^{\mathrm{n}}\,(1-x^2)^{\mathrm{n}/2}\,\frac{d^{\mathrm{n}}}{dx^{\mathrm{n}}}\,P_l(x), \tag{8}$$

where $P_l(x)$ are Legendre polynomials.

The rotation matrices are defined by

$$R^{(l)}_{\mathrm{nm}}(\alpha,\beta,\gamma) = e^{-\mathrm{i}\, n\alpha}\, r^{(l)}_{\mathrm{nm}}(\beta)\, e^{-\mathrm{i\,m}\gamma}, \tag{9}$$

where from the Wigner formula,

$$\begin{aligned} r^{(l)}_{\mathrm{nm}} \;=\; & \sum_t (-1)^t \frac{\sqrt{(l+\mathrm{n})!\,(l-\mathrm{n})!\,(l+\mathrm{m})!\,(l-\mathrm{m})!}}{(l+\mathrm{n}-t)!\,(l-\mathrm{m}-t)!\,t!\,(t-\mathrm{n}+\mathrm{m})!} \\ & \times\left[\cos\left(\frac{1}{2}\beta\right)\right]^{2l+\mathrm{n}-\mathrm{m}-2t} \times\left[\sin\left(\frac{1}{2}\beta\right)\right]^{2t-\mathrm{n}+\mathrm{m}} \end{aligned} \tag{10}$$

In Eq. (10), the summation extends over all integer values of t for which the arguments of the factorials are positive or zero. The number of terms in this sum is $1+\eta$, where η is the smallest of the four numbers $l\pm$n and $l\pm$m (c.f., Messiah 1962).

To evaluate the Stokes parameters of the scattered light, we note that in Eq. (2) the scattering function factors can be expressed as

$$1+\cos^2\theta = \frac{4}{3}\left[\sqrt{4\pi}\, Y^*_{00} + \sqrt{\frac{\pi}{5}}\, Y^*_{20}(\theta)\right] \tag{11}$$

and

$$\sin^2\theta\, e^{-2\mathrm{i}\phi} = 4\sqrt{\frac{2\pi}{15}}\, Y^*_{22}(\theta,\phi). \tag{12}$$

Substitution of Eqs. (11) and (12) into (2) and (1) and use of the orthogonality properties of the spherical harmonics yield

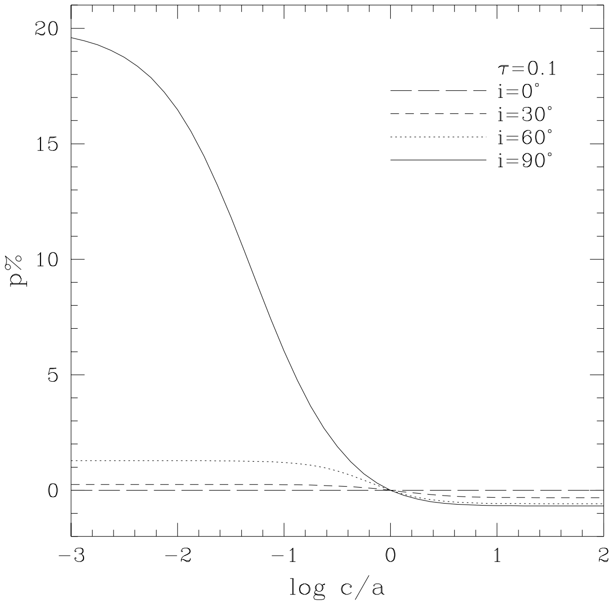

Fig. 3. The percentage normalized polarization p for MacLaurin spheroids (oblate shapes, $c<1$), and Jacobi ellipsoids (prolate shapes, $c>1$). The other two axes of the star are taken as $a=b=1$. The viewing perspective is for $\phi_{\mathrm{s}}=0°$, but different inclinations i as indicated. The envelope has an optical depth of $\tau=0.1$.

$$\begin{aligned}\mathcal{F}_{\mathrm{sc}} \;=\; & \frac{\sigma}{4\pi\, D^2}\,\Bigg[\sqrt{4\pi}\, R^{(0)}_{00}(\alpha,\beta,\gamma)\,\Gamma_{00} \\ & +\sqrt{\frac{\pi}{5}}\sum_{\mathrm{m}=-2}^{\mathrm{m}=2} R^{(2)}_{0\mathrm{m}}(\alpha,\beta,\gamma)\,\Gamma_{2\mathrm{m}}\Bigg]\end{aligned} \tag{13}$$

and

$$Z^* = \frac{3\sigma}{4\pi\, D^2}\sqrt{\frac{2\pi}{15}}\sum_{\mathrm{m}=-2}^{\mathrm{m}=2} R^{(2)}_{2\mathrm{m}}(\alpha,\beta,\gamma)\,\Gamma_{2\mathrm{m}} \tag{14}$$

where

$$\Gamma_{l\mathrm{m}} = \int_0^{\infty} n(r)\, F_{l\mathrm{m}}(r)\, r^2\, dr, \tag{15}$$

and

$$F_{l\mathrm{m}}(r) = \int_0^{\pi}\int_0^{2\pi} \mathcal{F}(r,\vartheta,\varphi)\, Y^*_{l\mathrm{m}}(\vartheta,\varphi)\, d\varphi\, \sin\vartheta\, d\vartheta. \tag{16}$$

The above expressions are exact and allow calculation of the scattered flux and Stokes parameters for any $\mathcal{F}(r,\theta,\phi)$, noting that all the harmonics of the order l or $|\mathrm{m}|$ higher than 2 are zero for the case of Thomson and Rayleigh scattering. If the star radiates isotropically, it is at once clear that Q and U will reduce to zero, and that $\mathcal{F}_{\mathrm{sc}}$ will only depend on the constant Γ_{00} term in Eq. (13). However in general, the degree and direction of polarization will depend on the properties of the coefficients $\Gamma_{l\mathrm{m}}$ describing the anisotropy of the source.

3. The case of an ellipsoidal star

In the case of a black body star of uniform surface temperature, the surface intensity is isotropic. Since we assume the

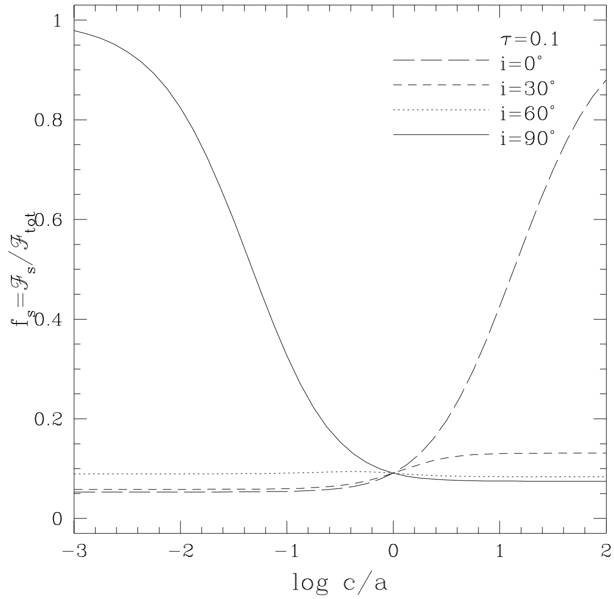

Fig. 4. The normalized scattered flux f_s for MacLaurin spheroids as in Fig. 3.

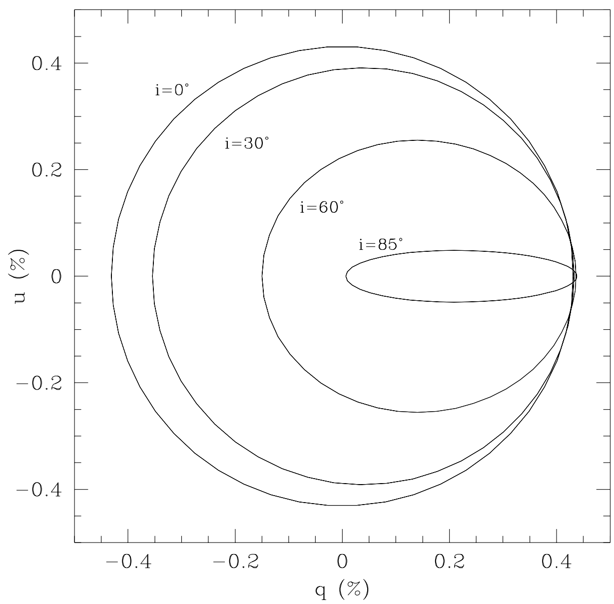

Fig. 5. Plot of qu-plane locus for a rotating binary with parameters $b = 2$, $a = c = 1$, and $i = 0°$, $30°$, $60°$, and $85°$.

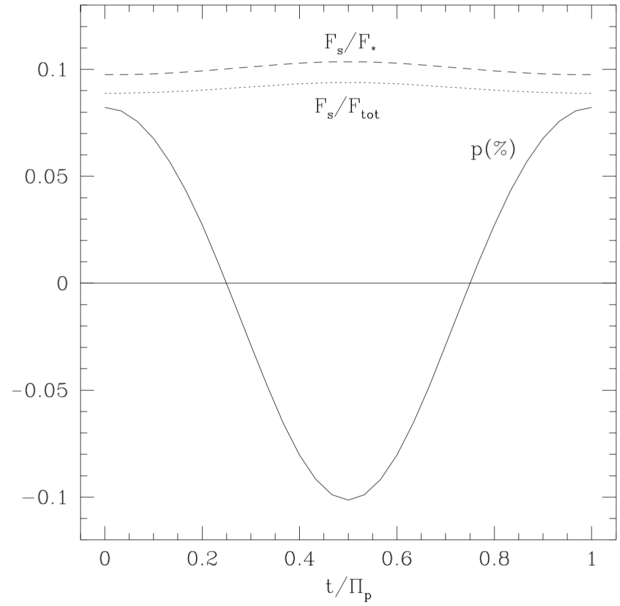

Fig. 6. Plot of p and f_s with the time as t/Π_p, for a non-rotating star having an oscillation along the b-axis with pulsation period Π_p, fractional amplitude $\delta = 0.1$, and phase $\Delta = 0$. See text for discussion.

envelope is large $(r \gg R)$, we treat the illumination as being radially directed only and express the incident flux in terms of the star's projected area $A_*(\vartheta, \varphi)$ as seen by the scattering element located at (r, ϑ, φ). The incident stellar radiation field is thus given by

$$\mathcal{F}(r, \vartheta, \varphi) \approx I_* \, \Delta\Omega = I_* \, \frac{A_*(\vartheta, \varphi)}{r^2}, \tag{17}$$

where I_* is the isotropic intensity of the stellar surface and $\Delta\Omega$ is the solid angle subtended by the source at the scatterer. For an ellipsoidal star with axes (a, b, c) along OX, OY, and OZ, respectively (see Fig. 2), the projected area is (c.f., Al-Malki 1992)

$$A_* = \pi \left| \sqrt{(bc\lambda)^2 + (ac\mu)^2 + (ab\nu)^2} \right|, \tag{18}$$

where $(\lambda, \mu, \nu) = (\cos\varphi \sin\vartheta, \sin\varphi \sin\vartheta, \cos\vartheta)$.

Inserting Eqs. (17) and (18) into Eq. (16), we obtain the expression

$$\Gamma_{l\mathrm{m}} = I_* \, N \, f_{l\mathrm{m}} \tag{19}$$

where the column density

$$N = \int_0^\infty n(r) \, dr \tag{20}$$

and the coefficient

$$f_{l\mathrm{m}} = \int_0^\pi \int_0^{2\pi} A_*(\vartheta, \varphi) \, Y^*_{l\mathrm{m}}(\vartheta, \varphi) \, d\varphi \sin\vartheta \, d\vartheta. \tag{21}$$

Note that the values of $f_{l\mathrm{m}}$ are now functions of the star's shape and size only (i.e., of a, b, and c). From symmetry it is clear that $f_{21} = f_{2,-1} = 0$, and $f_{22} = f_{2,-2}$. The terms $f_{l\mathrm{m}}$ are real for $l = \mathrm{m} = 0$, $l = 2$ and m$= \pm 2, 0$. The $f_{l\mathrm{m}}$ values that relate to the stellar anisotropy play a similar role in determining the observed polarization as does the shape factor (γ) of Brown & McLean (1977) – the latter being related to the oblateness or prolateness of the envelope but the former to that of the star.

The scattered flux and Stokes parameters reduce to

$$\mathcal{F}_\mathrm{sc} = \frac{\tau \, I_*}{4\pi \, D^2} \left\{ \sqrt{4\pi} \, f_{00} + \sqrt{\frac{\pi}{5}} \left[\sqrt{\frac{3}{2}} \, f_{22} \, \sin^2 i \cos 2\phi_\mathrm{s} + \frac{1}{2} f_{20} \, (3\cos^2 i - 1) \right] \right\}. \tag{22}$$

and

$$Z^* = \frac{3\tau\, I_*}{4\pi\, D^2} \sqrt{\frac{2\pi}{15}} \left\{ \frac{1}{2} f_{22} \left[(1+\cos^2 i)\cos 2\phi_{\rm s} \right.\right.$$
$$\left.\left. -2{\rm i}\cos i \sin 2\phi_{\rm s} \right] + \sqrt{\frac{3}{8}} f_{20}\, \sin^2 i \right\}. \qquad (23)$$

where $\tau = \sigma N$ is the radial optical depth of the envelope, and we have substituted for $(\alpha, \beta, \gamma) = (0, i, \phi_{\rm s})$ to give $R^{(0)}_{00}(0, i, \phi_{\rm s}) = 1$.

For most practical applications (also in the observational situation), one is interested in the normalized scattered flux and Stokes parameters defined by $(f_{\rm s}, q, u) = (\mathcal{F}_{\rm sc}, Q, U)/\mathcal{F}_{\rm tot}$, where the total observed flux $\mathcal{F}_{\rm tot}$ includes both the scattered light and the direct starlight. This latter component is $\mathcal{F}_* = I_* A_*(i, \phi_{\rm s})/D^2$, where the projected area A_* is of course that seen by the observer. Thus, the total flux is given by

$$\mathcal{F}_{\rm tot} = \frac{I_*}{D^2} \left[A_*(i, \phi_{\rm s}) + \frac{D^2}{I_*} \mathcal{F}_{\rm sc} \right]. \qquad (24)$$

Using the normalized Stokes parameters, the degree of polarization is $p = \sqrt{q^2 + u^2}$ and the polarization position angle is $\phi_{\rm p} = \frac{1}{2}\tan^{-1}(u/q)$.

There are quite evident similarities between Eqs. (22) and (23) for the scattered light properties of an axisymmetric light source (i.e., when $a = b$) embedded in a spherical envelope when compared to the results of Brown & McLean (1977) for the scattered light properties of a spherical source embedded in an axisymmetric envelope. For an axisymmetric star, the factor $f_{l,{\rm m}} = 0$, hence from Eq. (23), U is identically zero and $Q \propto \sin^2 i$, just as in Brown & McLean. The main difference is the somewhat more complicated dependence on viewing inclination in the case of an anisotropic source, the reason being that the direct stellar flux varies with inclination, so that $q = Q/\mathcal{F}_{\rm tot}$ will not vary as $\sin^2 i$ in general but only when the scattered flux is considerably smaller than the direct stellar contribution. Note that the expressions derived here for an anisotropic source generalizes the work of Gnedin et al. (1976), which was a 2-dimensional model for ellipsoidal effects in close X-ray binaries. In the following the results for an ellipsoidal source are applied to cases involving distorted stars, binary stars, and pulsating stars.

4. Case studies for polarization from ellipsoidal stars

There are various mechanisms for effecting deviations of a star from spherical symmetry, thus providing an anisotropic source. Here we consider the examples of (a) a single fast rotating star, for which we approximate the star as an oblate ellipsoid, (b) a binary system in which the more luminous component has a zero velocity surface approximated by a prolate ellipsoid, and (c) non-radially oscillating stars, for which the ellipsoid axes are functions of time. In this latter case, no attempt will be made to accurately determine the oscillation modes of the star, but simply to assume that at any phase the star's shape can be represented by an ellipsoid.

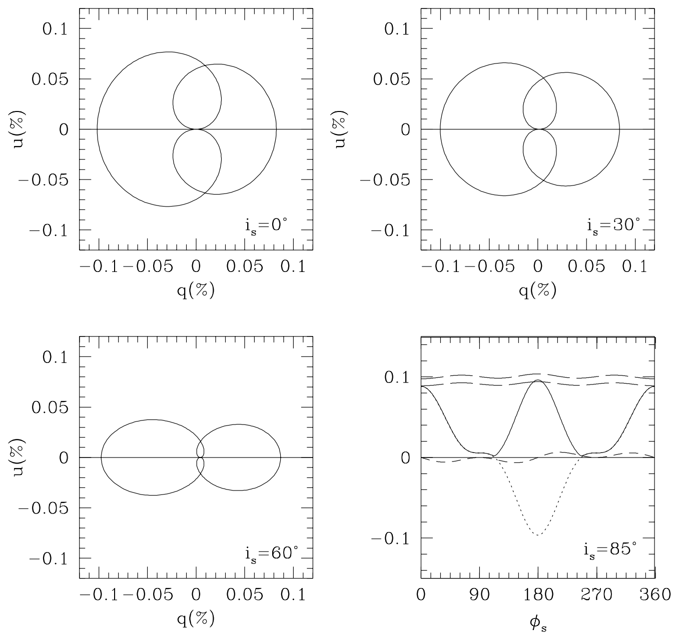

Fig. 7. The qu-plane locus for a full period of a rotating star with oscillation in b of $\delta = 0.1$, $\Delta = 0$, and $\omega_{\rm P} t = \phi_{\rm s}$ (i.e., the pulsation period equals the rotation period). The different cases are for inclinations $i = 0°$, $30°$, $60°$, and $85°$, as labeled. In the case of $i = 85°$, the flux and polarimetric variables are plotted against rotation phase, with solid being p, dotted q, short dash u, the upper long dashed line shows $f_{\rm s}$, and the lower long dashed line is $\mathcal{F}_{\rm sc}/\mathcal{F}_*$.

For illustration purposes we adopt a physically reasonable value for the envelope optical depth of $\tau = 0.1$. The degree of polarization does not scale linearly with optical depth unless the scattered light constitutes only a small fraction of the direct starlight. The latter is usually true in most cases of physical interest, but is not generally true when a, b, or c are small, in which case $\mathcal{F}_*$ may decrease quite rapidly as compared to $\mathcal{F}_{\rm sc}$.

The projected area A_* will be the primary factor in determining the polarization. We expect the maximum polarization to occur for cases of maximum scattered light and minimum projected area along the line of sight. In the extreme case of $A_* \to 0$ along the line of sight, $\mathcal{F}_* = 0$, $f_{\rm s} = 1$, and $(q, u) = (Q, U)/\mathcal{F}_{\rm sc}$. Note that for this case, the Stokes parameters become independent of the optical depth in the envelope. By symmetry the minimum polarization will be zero for any line of sight where the projected stellar area appears circular.

4.1. Oblate and prolate stars

Rotating stars can undergo considerable distortion. For models of main-sequence stars rotating near break-up speed, the expected distortion (in terms of equatorial to polar radius) for stars in uniform rotation is about 1.2 (Papaloizou & Whelan 1973; Tassoul 1978). Ostriker & Bodenheimer (1968) modeled rotating white dwarfs and showed that the distortion can be as large as 4. Such a value would produce a polarization of about 2.6% for an envelope with $\tau = 0.1$ (see Fig. 3).

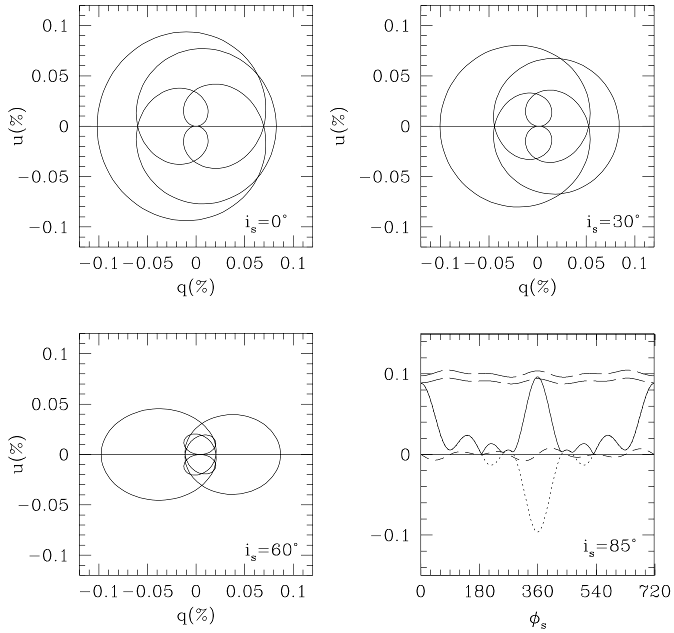

Fig. 8. As in Fig. 7, but for the case where the pulsation period is twice that of rotation. The plotted figure is for one pulsation period, corresponding to two rotation periods, hence the value of $\phi_{\rm s}$ extends to 720° instead of 360° as in the Figs. 7, 9, and 10.

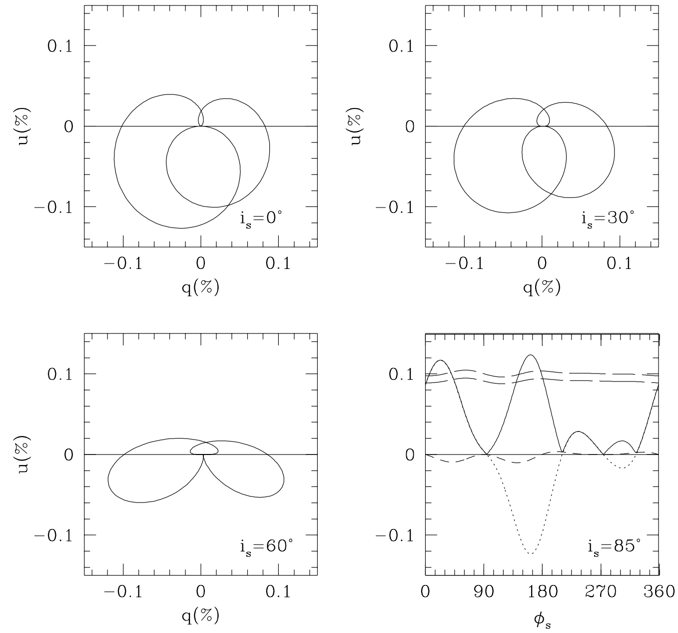

Fig. 10. With format similar to Fig. 7, a plot of polarization and $f_{\rm s}$ with time as $t/\Pi_{\rm p}$ for a rotating star, having oscillations in three axes: the a-axis with $\delta = 0.05$, $\Delta = \pi/2$, and $\omega_{\rm p} = 4\pi/\Pi_{\rm p}$; the b-axis with $\delta = 0.1$, $\Delta = 0$, and $\omega_{\rm p} = 2\pi/\Pi_{\rm p}$; and the c-axis with $\delta = 0.08$, $\Delta = \pi/2$, and $\omega_{\rm p} = 4\pi/\Pi_{\rm p}$. The cases for different viewing inclinations are indicated.

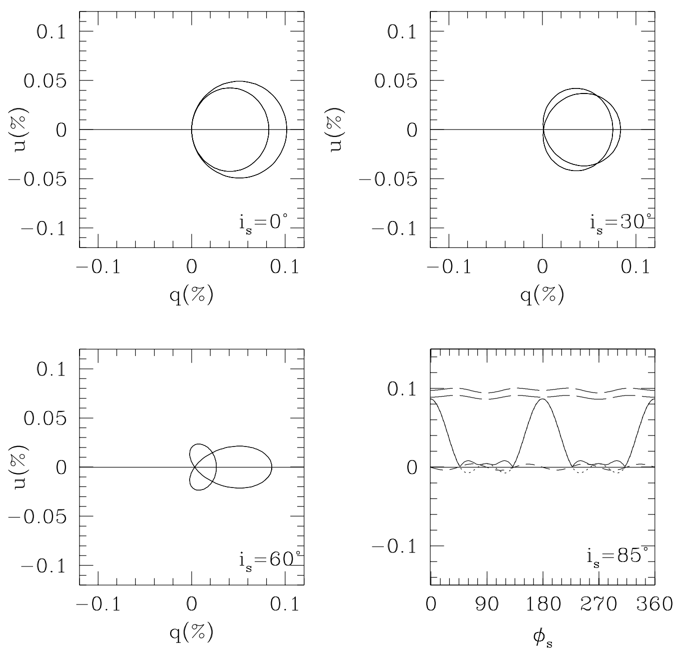

Fig. 9. As in Fig. 7, but for the case where the pulsation period is half that of rotation. The plotted figure is for one rotation period, corresponding to two pulsation periods.

The stable equilibrium configurations of rotating stars have been extensively studied (Chandrasekhar 1963; also Tassoul 1978 for a summary). Essentially, we may take the surfaces of equilibrium to be oblate (i.e., MacLaurin spheroids) or prolate (Jacobi) ellipsoids characterized by the values of their axes a, b, and c. Using Eqs. (22)–(24), the scattered flux and polarization of such models can be calculated.

Figs. 3 and 4 show the degree of polarization and the fractional scattered flux $\mathcal{F}_{\rm sc}/\mathcal{F}_{\rm tot}$ for ellipsoidal configurations in which $a = b$ and c (along the axis of rotation) is allowed to vary. Note that c is normalized to a. Curves are shown for different values of the inclination i (not to be confused with the complex number, i). Deviation from the $\sin^2 i$ behavior of the polarization (Brown & McLean 1977) results from the variation of the direct flux along the line of sight. For oblate stars the net polarization is perpendicular to the projection of the rotation axis on the sky, and for prolate it is parallel. Even with modest distortions, significant polarization is produced: for a star with $a = b = 1$, $c = 0.9$, and $\tau = 0.1$, the polarization p is about 0.1% at $i = 90°$.

From the above analysis, we calculate a maximum polarization of 20% for a flat disk star viewed edge on (i.e., $a = b = 1$, $c = 0.0$, $i = 90°$, and $\phi_{\rm s} = 0°$), for which zero projected stellar area will be observed so that the flux consists entirely of the scattered component and none from direct starlight. The maximum polarization is the same for any optical depth $\tau \lesssim 1$, because Z^* and $\mathcal{F}_{\rm tot} = \mathcal{F}_{\rm sc}$ both depend linearly on τ, which then disappears in the ratio for p.

4.2. Binary stars

The shape of a star filling its Roche lobe can be approximated by an ellipsoid (Chandrasekhar 1963; Gnedin et al. 1976; Bochkarev et al. 1979). The eccentricities of the ellipsoid will evidently depend on the masses of the stars and on their separation. However, stable equilibrium configurations can be expected to have a ratio of major to minor axes of up to 2 for typical mass ratios and separations (see Chandrasekhar 1963; Tassoul 1978).

For the extreme example of such binaries, consider one with $a = c$ and $b/a = 2$. Taking the envelope optical depth to be $\tau = 0.1$, the locus of q and u throughout the course of one orbital period (i.e., as $\phi_{\rm s}$ varies from 0 to 2π) is a circle for $i = 0°$, but becomes increasingly elliptical with more edge-on viewing inclinations, eventually degenerating to linear at $i = 90°$ (Fig. 5). The locus is described twice in one period. The normalized scattered flux $f_{\rm s}$ is constant at a value of 0.08 for a pole-on viewing perspective, increasing to a maximum as i approaches $90°$. The value of $f_{\rm s}$ peaks at 0.15 for $i = 90°$ and $\phi_{\rm s} = 90°$ or $\phi_{\rm s} = 270°$, phases that correspond to minimum direct stellar flux emitted into the line of sight.

4.3. Non-radially pulsating stars

As a simple model of a non-radially pulsating (NRP) star, we approximate the star's shape as a series of ellipsoids described by time varying axes a, b, and c. Such possible orthogonality in the oscillations was proposed by Serkowski (1970) in relation to his observation of RV Tau stars which showed a change in the brightness of about 5 magnitudes. Such variations will affect the scattered flux $\mathcal{F}_{\rm sc}$ as well as the direct flux $\mathcal{F}_*$, and result in an interesting time dependence of the polarization, both in value and position angle. It appears that many variable stars have this kind of oscillation (e.g., Omicron Ceti, W Vir, and RR Lyrae). The distortion from sphericity may be up to 90% (i.e., c/a or $b/a = 0.1$; see Sect. 4.1). A distortion of 20% adequately accounts for the typical polarimetric variation (Karovska et al. 1992 for Omicron Ceti).

Consider a non-rotating star that oscillates along the y-axis, and assume that $b = 1+\delta\cos(\omega_{\rm p}t+\Delta)$, where δ is the fractional distortion amplitude from spherical symmetry, $\omega_{\rm p} = 2\pi/\Pi_{\rm p}$ with $\Pi_{\rm p}$ the pulsation period, and Δ is the phase. We have taken $a = c$, and have accordingly normalized the b-axis. Fig. 6 shows the time variation in p and $f_{\rm s}$ for this kind of pulsation, when the star is at $\phi_{\rm s} = 0°$ or $180°$ (since the star is not rotating, $\phi_{\rm s}$ remains fixed). There is no inclination dependence here because the variations are along the b-axis, hence at a given time, the projected stellar area for $\phi_{\rm s} = 0°$ or $180°$ remains the same for any i. As the star goes from oblate to prolate, the polarization position angle undergoes a $90°$ rotation.

In the case of both stellar rotation and pulsation, the form of the variations in the Stokes parameters will in general also depend on the rotation period $\Pi_{\rm r}$. There are dynamical reasons to expect these periods to be related (Becker 1986). The polarization and scattered flux can be calculated from the results of Sect. 4.1, by taking $\phi_{\rm s} = \omega_{\rm r}t$ where $\omega_{\rm r} = 2\pi/\Pi_{\rm r}$.

We shall deal with three generic cases:

1. $\Pi_{\rm p} = \Pi_{\rm r}$. Fig. 7 plots the changes in the qu-plane in panels a, b, and c as the star rotates, and in 7d the variations of the flux and polarization with $\phi_{\rm s}$ is shown. We have taken $\Delta = 0$, $\delta = 0.1$, and $a = c$. Here the loci are double lobed owing to the changing shape of the star during rotation. The size of the lobes shrink in u with increasing i. Values of $f_{\rm s}$ are about 0.09 with only small variations.
2. $\Pi_{\rm p} = n\Pi_{\rm r}$. For integer n, the loci are described n times per pulsation period. Fig. 8 shows the qu variations for different inclinations with $n = 2$. This combined effect of rotation and pulsation may explain the multiple modes observed in some pulsating stars (e.g., β Cep [Becker 1986]). The pattern gets more complicated and shrinks in overall scale as i increases. Again, $f_{\rm s}$ has values of 0.09 with only small variations.
3. $\Pi_{\rm p} = \nu\Pi_{\rm r}$. Here $\nu = n/m$ is a rational number expressed in its lowest terms. The period in q and u will be $m\Pi_{\rm r}/2$. Fig. 9 shows the qu-loci for $\nu = 1/2$. If ν is an irrational number, then the qu-locus will not close.

The above analysis is easily generalized to pulsations along several axes. We will consider the case of stellar pulsation in three directions, using: an a-axis pulsation with $\delta = 0.05$, $\Delta = \pi/2$, and $\omega_{\rm p} = 4\pi/\Pi_{\rm p}$; b-axis pulsation with $\delta = 0.1$, $\Delta = 0$, and $\omega_{\rm p} = 2\pi/\Pi_{\rm p}$; and c-axis pulsation with $\delta = 0.08$, $\Delta = \pi/2$, and $\omega_{\rm p} = 4\pi/\Pi_{\rm p}$. The qu-loci for a rotating star of the above values is shown in Fig. 10. In general, the figures become more complicated as the number of oscillating axes increases, and the value of maximum p increases as well, but by a small factor. Evidently, as the number of parameters describing the variations in the stellar distortion and phase increases, so does the complexity of the behavior of p, q, u, and $f_{\rm s}$.

5. Conclusions

A model for anisotropic flux and Thomson or Rayleigh single scattering in spherical circumstellar envelopes has been derived, the analysis involving full use of the properties of spherical harmonics under rotations. Applications of the model to an ellipsoidal black body source shows that the highest possible polarization will be 20%, in which case the total observed flux is the scattered flux. This limit occurs for the pathological case of a star of zero projected area when viewed edge on; however, for more realistic cases, the expected polarization will be around 1% or smaller.

This study shows that the polarization produced by an ellipsoidal star with a spherical envelope is comparable to that from a spherical point source star with an ellipsoidal envelope (see Brown & McLean 1977). The degree of the polarization predicted by the model for physically reasonable distortions and electron densities in the scattering envelope are fully in accord with observations. For a single star that is not undergoing pulsations, this mechanism for producing polarization cannot be observationally distinguished from that proposed previously by Brown & McLean from polarization data alone. However, from spectroscopic measurements of line profiles, such a distinction could possibly be made.

The analysis presented here is easily generalized to more complicated anisotropic fluxes. We have concentrated on the anisotropies in the flux from the star that are produced by rotational distortion. The technique can be extended to study the consequences of spots on the stellar surface for the observed polarization. To isolate the effects of stellar anisotropy, we have here concentrated on the cases where the envelope is spherical. Generalization to include the more realistic case where there is also an aspherical circumstellar envelope will be presented in a future paper.

Acknowledgements. This work has been supported financially by the University of King Saud and by grants from PPARC.

References

Al-Malki M.B., 1992, Ph.D. Thesis, University of Glasgow
Becker S.A., 1986, In: Cox A.N., Sparks W.M., Starrfield S.G. (eds.) Stellar Pulsation. 16
Bjorkman J.E., Bjorkman K.S., 1994, ApJ 436, 818
Bochkarev N.G., Karitskaya E.A., Shakura N.I., 1979, SvA 23, 8
Brown J.C., McLean I.S., 1977, A&A 57, 141
Brown J.C., McLean I.S., Emslie A.G., 1978 A&A 68, 415
Brown J.C., Carlaw V.A., Cassinelli J.P., 1989, ApJ 344, 341
Brown J.C., Fox G.K., 1989, ApJ 347, 468
Cassinelli J.P., Nordsieck K.H., Murison M.A., 1987, ApJ 317, 293
Chandrasekhar S., 1963, ApJ 138, 1182
Collins G.W., II., Buerger P.F., 1974, In: Gehrels T. (ed.) Planets, Stars, and Nebulae Studied with Photopolarimetry. University of Arizona Press, 663
Fox G.K., 1991, ApJ 379, 663
Fox G.K., 1993, MNRAS 260, 513
Fox G.K., Brown J.C., 1991, ApJ 375, 300
Gnedin Yu.N., Silant'ev N.A., Shibanov Yu.A., 1976, SvA 20, 530
Haisch B.M., Cassinelli J.P., 1976, ApJ 208, 253
Jackson J.D., 1975, Classical Electrodynamics. 2nd ed., J. Wiley & Son, New York
Karovska M., Nisenson P., Papaliolios C., 1992, Sky & Telescope 83, 130
Messiah A., 1962, Quantum Mechanics VII, North-Holland Publishing Company, Amsterdam
Milgrom M., 1978, A&A 65, L1
Ostriker J.P., Bodenheimer P., 1968, ApJ 151, 1089
Papaloizou J.C.B., Whelan J.A.J., 1973, MNRAS 164, 1
Rudy R.J., Kemp J.C., 1978, ApJ 221, 220
Serkowski K., 1970, ApJ 160, 1107
Simmons J.F.L., 1982, MNRAS 200, 91
Simmons J.F.L., 1983, MNRAS 205, 153
Stamford P.A., Watson R.D., 1980, Acta Astron. 30, 193
Tassoul J.L., 1978, Theory of Rotating Stars. Princeton University Press, Princeton, New Jersey, USA
van de Hulst H.C., 1957, Light Scattering by Small Particles. J. Wiley & Son, New York